ORNL/CP-95872

CONF-9706232--

Measurement of Optical Properties of Small Particles

E. T. Arakawa, P. S. Tuminello
Life Sciences Division, Oak Ridge National Laboratory
Oak Ridge, TN 37831

B. N. Khare
NASA Ames Research Center
Moffett Field, CA 94035

M. E. Milham
USAMCCOM, Edgewood Research, Development, and Engineering Center
Aberdeen Proving Ground, MD 21010

S. Authier
Ecole Superiere d'Optique
91403 Orsay Cedex, France

J. Pierce
Science Alliance, University of Tennessee
Knoxville, TN 37996

1997 Scientific Conference on Obscuration and Aerosol Research
Aberdeen Proving Ground, Maryland
June 23–26, 1997

Abstract. We have measured the optical constants of montmorillonite and the separated coats and cores of *B. subtilis* spores over the wavelength interval from 200 nm to 2500 nm. The optical constants of kaolin were obtained over the wavelength interval from 130 nm to 2500 nm. Our results are applicable to the development of systems for detection of airborne biological contaminants. Future work will include measurement of the optical constants of *B. cereus* spores, *B. subtilis* vegetative cells, egg albumin, illite, and a mixture (by weight) of one-third kaolin, one-third montmorillonite, and one-third illite.

I. INTRODUCTION

The U. S. Army Edgewood Research, Development and Engineering Center (ERDEC) required values of the optical constants of several biological and inorganic materials from the ultraviolet to the near-infrared spectral region for modeling studies of biological detection schemes at ERDEC. We were contracted by ERDEC to determine optimal sample preparation and spectroscopic methods for obtaining accurate values of the optical constants of two soil-derived mineral samples, montmorillonite and kaolin, and two samples of biological origin, separated coats and cores of *Bacillus subtilis* spores (Auxotrophic Strain 1A1). These techniques were to include measurements of spectral reflectance and transmittance of the samples, and appropriate analytical techniques, such as Kramers-Krönig analysis, for obtaining optical constants from the experimental data throughout the required spectral region from 200 nm (50,000 cm^{-1}) to 2500 nm (4000 cm^{-1}), with the highest quality data needed in the short wavelength (high wavenumber) region from 200 nm (50,000 cm^{-1}) to 333 nm (30,000 cm^{-1}).

II. EXPERIMENTAL

Using techniques previously applied with success in our laboratory, we have measured the real (n) and imaginary (k) parts of the complex refractive index $N = n + ik$ of montmorillonite, kaolin, and separated coats and cores of *B. subtilis* spores over the spectral range 200 nm to 2500 nm. Care was taken to insure that high quality values of the optical constants were obtained in the short wavelength (high wavenumber) region from 200 nm to 333 nm. All measurements were performed at room temperature.

A. Montmorillonite

1. Sample preparation

Montmorillonite is a naturally occurring mineral with chemical formula $(Al, Mg)_8(Si_4O_{10})_3 \cdot (OH)_{10} \cdot 12H_2O$. The sample, Montmorillonite K 10, a white powder, was obtained from Aldrich Chemical Company. Thin films of montmorillonite were vacuum-evaporated onto glass and CaF_2 substrates in a diffusion-pumped chamber. The sample was heated in a Ta boat to 1500 C. Half of the face of the substrates were masked in order for the transmission of the bare substrate to be measured. The base pressure in the evaporator was in the 10^{-5} torr range. The film thickness was measured with a quartz crystal thickness monitor.

2. Optical Constants Measurements

a. Extinction Coefficient k

The extinction coefficient of montmorillonite was obtained from transmission measurements made on thin films of montmorillonite on glass and CaF_2 substrates. Transmission spectra were obtained using a modernized Cary 14

DISCLAIMER

spectrophotometer which had been interfaced to a personal computer for data acquisition and analysis. The extinction coefficient for the montmorillonite films was calculated using

$$k = \frac{\lambda \ln(T_s / T)}{4\pi t} \tag{1}$$

where λ is the wavelength, T is the transmittance of the of the film-substrate system, T_s is the transmittance of the bare substrate, and t is the thickness of the film. Transmission spectra of the films were obtained over the wavelength interval from 200 nm to 2500 nm. A representative transmittance spectrum of a montmorillonite film is shown in Fig. 1. The oscillations are due to interference of light multiply reflected from the front and rear surfaces of the montmorillonite film. In spectral regions where oscillations were present, T_s used in Eq. 1 was chosen to be the value of envelopes drawn through the maxima of the measured transmittance. Film thicknesses were obtained from the positions of interference maxima and minima in plots of film transmittance as a function of wavelength (Harrick 1971). Thicknesses obtained using this method were found to be more accurate than those indicated by the thickness monitor at the completion of an evaporation.

b. Index of Refraction n

The index of refraction of montmorillonite was obtained from a Kramers-Krönig (KK) inversion of the data for k. The KK relation between n and k, given by the dispersion relation (Stern 1963)

$$n(E) = 1 + \frac{2}{\pi} \int_0^{\infty} \frac{E' k(E')}{(E')^2 - E^2} dE' \tag{2}$$

where E is the photon energy, was used to obtain n over the wavelength interval 200 nm to 2500 nm. The k values used as input for the KK analysis were chosen as follows. In the wavelength interval 200 to 2500 nm, k obtained from transmission measurements described above were used. For the region 2500 nm $\leq \lambda \leq$ 100 μm, we used a constant value of k, equal to the value at $\lambda = 2500$ nm. The low-energy integration in Eq. (2) was truncated at 100 μm, since the contribution to the integral for wavelengths above 100 μm has no significant effect on the n values in the region of interest. For wavelengths below 200 nm, the lower limit of our transmission measurements, we used our previously determined values for kaolin (described below). A high-energy cutoff for the integration of 24 eV was chosen to make the calculated KK values of n agree with independently measured values in the 300 nm to 650 nm region. These independent n values were obtained from measurements of the critical angle at a sapphire-sample interface. In this technique, a montmorillonite film is vacuum-evaporated onto the flat face of a sapphire semicylinder. The reflectance of the sapphire-sample interface is measured as a function of incident angle. Fresnel's equations as a function of angle of incidence are used to obtain the best values of n and k which fit the experimental data. A typical reflectance spectrum obtained using this technique is presented in Fig. 2.

The index of refraction of montmorillonite was also obtained at different wavelengths using a method described by Abeles (1950) for thin films on thick substrates. In this experiment, reflectance as a function of incident angle is measured for a montmorillonite film on a sapphire semicylinder or a thick glass substrate. This reflectance is plotted along with that of the uncoated surface. The intersection of the two curves yields Brewster's angle for the film. The film index is obtained from this angle using the equation

$$n = \tan \theta_B \qquad (3)$$

Typical reflectance data obtained using this method are shown in Fig. 3. The index of refraction and extinction coefficient of montmorillonite determined in this study are shown in Fig. 4 and tabulated in Table I. In the plot of k, the solid curve represents the averaged result of our transmission measurements. The solid curve for n is the result of the KK analysis on k. The individual points plotted for n are the results of the independent measurements using the critical-angle and Brewster-angle techniques.

B. Kaolin

1. Sample preparation

Kaolin is a clay, or more specifically, a hydrated aluminum silicate known as kaolinite. Its chemical formula is $Al_4(Si_4O_{10})(OH)_8$. In powdered form, kaolin particles are white and 0.1 to 4 microns in diameter. Its abundance in the atmosphere is sufficiently large that one author refers to it as a "nuisance dust" (Lewis, 1993).

Kaolin films were prepared by thermally evaporating the powdered form of the material onto glass, quartz, and CaF_2 substrates 1 inch in diameter and 2 mm thick in the evaporation chamber described above. Films were also evaporated onto the flat face of sapphire and suprasil semicylinders. The substrates were placed 15 cm above a Ta boat. A shield could be held in place between the evaporant and the substrates. The current passing through the boat was kept low until all adsorbed water had escaped from the evaporant. It is important to note that water is also lost from kaolin *molecules* near 450 C (Lewis, 1993). After this water had been removed, the shield was moved away and the evaporation begun. From its white color it was determined that the temperature of the boat reached 1500 C.

2. Optical Constants Measurements

a. Extinction coefficient k

The extinction coefficient of kaolin was obtained from transmission measurements made on thin films of kaolin on glass, quartz, and CaF_2 substrates over the wavelength interval from 130 nm to 400 nm. In the region from 400 nm to 2500 nm, the transmittance of kaolin in index matching fluid ($n = 1.532$ at 500 nm) was measured. Transmission spectra were obtained using the Cary 14 spectrophotometer and a Seya-Namioka vacuum-ultraviolet monochromator (McPherson model 235). The extinction coefficient for the kaolin films was calculated using Eq. 1. Film thicknesses were obtained from the positions of interference maxima and minima in plots of film transmittance as a function of wavelength.

b. Index of refraction *n*

The KK relation between *n* and *k* (Eq. 2) was used to obtain *n* over the wavelength interval 130 nm to 2500 nm. The *k* values used as input for the KK analysis were chosen as follows. In the wavelength interval 130 to 2500 nm, *k* obtained from our transmission measurements were used. For the region 2500 nm $\leq \lambda \leq$ 100 μm, we used a constant value of *k*, equal to the value at $\lambda = 2500$ nm. The low-energy integration was truncated at 100 μm. For wavelengths below 130 nm, the lower limit of our transmission measurements, we used our previously determined values for Titan tholin (Khare *et al.*, 1984, Sagan *et al.*, 1992), a complex organic solid produced from plasma discharge irradiation in an N_2/CH_4 atmosphere containing 10% CH_4. The extinction coefficient of Titan tholin joined smoothly onto our *k* values for kaolin below 130 nm. A high-energy cutoff for the integration of 45 eV was chosen to make the calculated KK values of *n* agree with independently measured values in the 260 nm to 600 nm region. These independent *n* values were obtained using the critical-angle and Brewster-angle techniques.

The index of refraction and extinction coefficient of kaolin determined in this study are shown in Fig. 5 and tabulated in Table II. The nomenclature used for presentation of the data shown in Fig. 5 is the same as that of Fig. 4.

C. Separated Coats of *B. subtilis* Spores

1. Sample preparation

Separation of the *B. subtilis* spore coats was performed by Sharon Bilotta of Cornell University. A small quantity of the original purified, compressed spore pellet was suspended in sterile water and plated on nutrient medium to ensure the viability of the spores. Two days later, the plates showed flourishing growth, typical of *B. subtilis.* A portion of the remaining pellet was suspended in distilled water. The suspension was beaten in a Mini-Beadbeater (Biospec Products, Bartlesville OK) for two minutes and then examined in a phase-contrast microscope for breakage of the spores. Approximately half of the spores were broken. The sample was then beaten for another 50 seconds; microscopic inspection revealed that approximately 96% of the spores were broken. The sample was then spun at 3300 rpm in a microcentrifuge for 5 minutes to separate the heavier coat from the rest of the spore. The resulting pellet was frozen and maintained in liquid nitrogen. The sample was transported in this frozen state to our laboratory in Oak Ridge. The separated spore components were stored in a freezer at –78 C.

A small amount of the frozen sample of *B. subtilis* coats in water, as received from Cornell, was allowed to melt and dry at room temperature. Three-hundred micrograms of dried coats was dissolved in 20 μl of triply-distilled water to obtain a 15 μg/μl solution. Other solutions having concentrations of 10 μg/μl and 20 μg/μl were prepared and used in transmission measurements. To obtain complete mixing, all solutions were shaken for two hours using a Vortex Jr. mixer (Scientific Industries, Inc., Springfield, MA 01103).

2. Optical Constants Measurements

a. Extinction coefficient *k*

The extinction coefficient of *B. subtilis* spore coats was obtained from transmission measurements made on the solutions in water. A thin cell with CaF_2 windows was used in the measurements. A cell thickness of 142 μm was determined from a plot of the interference pattern obtained from a measurement of the transmission of the empty cell as a function of wavelength. Values for the extinction coefficient *k* were obtained using

$$k = \frac{\lambda \ln(T_{water}/T)}{4\pi t} \tag{4}$$

where λ is the wavelength, T is the transmittance of the of the cell filled with the sample solution, T_{water} is the transmittance of the cell filled with water, and t is the equivalent thickness of the spore coats. The equivalent thickness was obtained from

$$t = \frac{\text{concentration} \times \text{pathlength}}{\text{density}} \tag{5}$$

where the pathlength is 142 μm. Using the sink-float method, the density of the spore cores was found to be 1.21 ± 0.01 g/cm^3. Several solutions of sucrose in water were prepared with densities varying in increments of 0.01 g/cm^3. Small dried pieces of spore coats were placed on the surfaces of these solutions. With the aid of a low-power microscope, the particles could be seen either floating on the surface, sinking to the bottom, or suspended below the surface, depending on the concentration of the sucrose solution.

b. Index of refraction *n*

The KK relation between *n* and *k* (Eq. 2) was used to obtain *n* over the wavelength interval 200 to 2500 nm. The *k* values used as input for the KK analysis were chosen as follows. In the wavelength interval 200 to 2500 nm, *k* obtained from transmission measurements described above were used. For the region 2500 nm $\leq \lambda \leq$ 100 μm, we used a constant value of *k*, equal to the value at λ=2500 nm. The low-energy integration in Eq. (2) was truncated at 100 μm. For wavelengths below 200 nm, we used our previously determined values for Titan tholin. These were smoothly joined onto our *k* values for the spore coats. A high-energy cutoff for the integration of 37 eV was chosen to make the calculated KK values of *n* agree with independently measured values in the 300 to 650 nm region. These independent *n* values were obtained using the critical-angle and Brewster-angle techniques.

The index of refraction and extinction coefficient of separated coats of *B. subtilis* spores determined in this study are shown in Fig. 6 and tabulated in Table III. The nomenclature used for presentation of the data shown in Fig. 6 is the same as that of Fig. 5.

D. Separated Cores of *B. subtilis* Spores

1. Sample preparation

The spore core sample was removed from the freezer and allowed to melt in its vial at room temperature. The vial containing the melted sample was placed in a VWR Vortexer 2 (Scientific Industries, Inc., Bohemia, NY 11716) and shaken for 5 minutes. One-hundred microliters of the sample was placed in an empty vial and allowed to dry at room temperature. After drying, the vial was weighed on a Mettler UMT2 microbalance (Mettler Instrument Corp., Hightstown, NJ 08520). The concentration of the sample as received from Cornell was found to be 0.77 μg/μl. A higher concentration was needed for useful transmission measurements. The concentration was increased by placing 200 μl of the original sample, obtained from the bottom of the vial, in another empty vial and allowed to dry. This vial was weighed after drying and contained 395 μg of sample. A volume of 26.33 μl of triply-distilled water was added to the vial to obtain a sample concentration of 15 μg/μl. This sample was shaken in the Vortex Jr. mixer for 2 hours to obtain complete mixing. Other samples having concentrations of 1.975 μg/μl and 3.85 μg/μl were made in a similar manner.

2. Optical Constants Measurements

a. Extinction Coefficient k

Transmittance of pure water and the spore core solutions in water was measured using the Cary 14 spectrophotometer over the wavelength interval 200 to 2500 nm. The samples were placed in the thin cell with CaF_2 windows. Values for the extinction coefficient k were obtained using Eq. 4. Using the sink-float method, the density of the spore cores was 1.20 g/cm^3.

b. Index of Refraction n

The KK relation between n and k (Eq. 2) was used to obtain n over the wavelength interval 200 to 2500 nm. The k values used as input for the KK analysis were chosen in a manner similar to that of the spore coats. A high-energy cutoff for the integration of 31 eV was chosen to make the calculated KK values of n agree with independently measured values obtained using the critical-angle and Brewster-angle techniques in the 250 to 650 nm region.

The index of refraction and extinction coefficient of separated cores of *B. subtilis* spores determined in this study are shown in Fig. 7 and tabulated in Table IV. The nomenclature used for presentation of the data shown in Fig. 7 is the same as that of Fig. 6.

III. DISCUSSION

For the materials covered in many studies, the particle sizes in inhomogeneous samples are comparable to the wavelengths of light used in measurements of reflectance or transmittance. This is often the case at short wavelengths in the UV and visible spectral regions. It is important to note that standard techniques for measuring optical constants can be used only on samples of optical quality films that eliminate scattering. This criterion was fulfilled for all materials discussed in this investigation. Our thin films of montmorillonite and kaolin prepared by thermal evaporation were smooth and yielded easily discernible interference patterns. Fig. 1 shows the measured transmittance (solid line) of a montmorillonite film 0.66 μm thick. The transmittance calculated using the measured optical constants in the exact equation for transmittance as a function of n and k (dashed line) reproduces the measured spectrum well and confirms the accuracy of our measurements. Scattering was reduced for the solutions of *B. subtilis* spore coats and cores by using a solvent (water) which has an index of refraction comparable to that of the spore coats and cores.

The optical constants of montmorillonite, kaolin, and 22 other rocks and minerals were obtained by Egan and Hilgeman (1979) by measuring total diffuse reflectance and transmittance from thin sections and pressed pellets and using a scattering theory to determine the extinction coefficient of the samples. These investigators were not able to collect a large fraction of the scattered light and thus obtained k values which were too small. Their kaolin k values, when multiplied by a constant (approximately 25), join smoothly onto ours below 550 nm. In their table of the optical constants of kaolin, the values of n are generally too low. For example, at $\lambda = 600$ nm, R is 0.501 and the value of n derived from scattering theory is 1.493 compared with our value of 1.568.

The magnitude of our experimental errors is difficult to evaluate. The uncertainty in all transmission measurements is estimated to be 2%. In the measurements of the extinction coefficient of solid films of montmorillonite and kaolin, the thicknesses of the films were obtained from the maxima and minima in plots of transmittance as a function of wavelength. Errors present in these thickness measurements tended to cancel since the extinction coefficients obtained from several films of different thickness were averaged in order to obtain the final k values. The error in the extinction coefficient for montmorillonite and kaolin presented here is estimated to be 3%. In the measurement of the extinction coefficient of spore coats and cores, the sample thickness was always 142 μm, the thickness of the thin transmission cell. Since this value is highly accurate, error in the pathlength used in Eq. 5 is very small. For the spore coats and cores solutions in water, errors in the measurement of the mass of the dry sample and volume of water used to prepare the solutions were small (less than 1% for each). The error in the density measurements of the spore coats and cores is approximately 1%. The total error in the extinction coefficient of the spore coats and cores is estimated to be 3%.

The error in the measurement of the index of refraction using the critical-angle technique is primarily due to imperfect fitting of the experimental data and the theoretical reflectance calculated using Fresnel's equations (see Fig. 2). This error results in an absolute error in the index of refraction of approximately 0.005 for the index range of the materials in this study.

The present work is applicable to the development of systems for detection of airborne biological contaminants. The optical properties of the components of the background dust particles are needed in order to separate their contribution to a signal received by such a detection system. Future work will include measurement of the optical constants of *B. cereus* spores, *B. subtilis* vegetative cells, egg albumin, illite, and a mixture (by weight) of one-third kaolin, one-third montmorillonite, and one-third illite.

Acknowledgments

This work was supported by the Edgewood Research, Development And Engineering Center (Mr. Merrill E. Milham) under the auspices of the U. S. Army Research Office Scientific Services Program administered by Battelle (Contract No. SSP96–18). Also sponsored by the Office of Health and Environmental Research, U. S. Department of Energy under contract DE–AC05–96OR22464 with Lockheed Martin Energy Research Corp.

REFERENCES

Abeles, F., J. Phys. Radium **11**, 310 (1950).

Egan, W. G., and T. W. Hilgeman, "Optical Properties of Inhomogeneous Materials; Applications to Geology, Astronomy, Chemistry, and Engineering," New York: Academic Press (1979).

Harrick, N. J., "Determination of Refractive Index and Film Thickness from Interference Fringes," Appl. Opt. **10**, 2344–2349 (1971).

Khare, B. N., C. Sagan, E. T. Arakawa, F. Suits, T. A. Callcott, and M. W. Williams, Icarus **60**, 127 (1984).

Lewis, R., "Hazardous Chemicals Desk Reference," New York: Van Nostrand Reinhold (1993), p. 751.

Sagan, C., W. R. Thompson, and B. N. Khare, *Acct. Chem. Res.* **25**, 286 (1992).

F. Stern, Elementary Theory of the Optical Properties of Solids, in "Solid State Physics, Vol. 15," edited by F. Seitz and D. Turnbull, Academic Press, New York, 1963, pp. 229–408.

Table I. Real (*n*) and imaginary (*k*) parts of the complex refractive index of montmorillonite.

λ (μm)	*n*	*k*	λ (μm)	*n*	*k*
0.20	1.777	0.142	0.72	1.527	0.00138
0.21	1.748	0.107	0.73	1.526	0.00136
0.22	1.723	0.0838	0.74	1.526	0.00134
0.23	1.702	0.0636	0.75	1.526	0.00132
0.24	1.680	0.0489	0.76	1.525	0.00130
0.25	1.662	0.0411	0.77	1.525	0.00128
0.26	1.648	0.0356	0.78	1.525	0.00126
0.27	1.637	0.0300	0.79	1.524	0.00125
0.28	1.626	0.0250	0.80	1.524	0.00124
0.29	1.617	0.0220	0.81	1.524	0.00123
0.30	1.609	0.0190	0.82	1.524	0.00122
0.31	1.602	0.0170	0.83	1.523	0.00121
0.32	1.596	0.0150	0.84	1.523	0.00120
0.33	1.590	0.0130	0.85	1.523	0.00120
0.34	1.585	0.0110	0.86	1.523	0.00120
0.35	1.580	0.0100	0.87	1.522	0.00120
0.36	1.576	0.00900	0.88	1.522	0.00119
0.37	1.572	0.00800	0.89	1.522	0.00119
0.38	1.569	0.00700	0.90	1.522	0.00119
0.39	1.565	0.00650	0.91	1.521	0.00118
0.40	1.562	0.00600	0.92	1.521	0.00118
0.41	1.560	0.00550	0.93	1.521	0.00117
0.42	1.557	0.00500	0.94	1.521	0.00117
0.43	1.555	0.00450	0.95	1.521	0.00116
0.44	1.553	0.00420	0.96	1.521	0.00116
0.45	1.551	0.00400	0.97	1.521	0.00115
0.46	1.549	0.00370	0.98	1.520	0.00114
0.47	1.547	0.00350	0.99	1.520	0.00113
0.48	1.546	0.00320	1.00	1.520	0.00113
0.49	1.544	0.00300	1.01	1.520	0.00113
0.50	1.543	0.00280	1.02	1.520	0.00114
0.51	1.542	0.00270	1.03	1.520	0.00114
0.52	1.541	0.00253	1.04	1.520	0.00114
0.53	1.540	0.00238	1.05	1.519	0.00114
0.54	1.538	0.00223	1.06	1.519	0.00114
0.55	1.537	0.00213	1.07	1.519	0.00114
0.56	1.536	0.00206	1.08	1.519	0.00114
0.57	1.535	0.00200	1.09	1.519	0.00113
0.58	1.535	0.00195	1.10	1.519	0.00113
0.59	1.534	0.00190	1.11	1.519	0.00113
0.60	1.533	0.00185	1.12	1.519	0.00113
0.61	1.532	0.00180	1.13	1.518	0.00113
0.62	1.532	0.00175	1.14	1.518	0.00113
0.63	1.531	0.00170	1.15	1.518	0.00113
0.64	1.531	0.00165	1.16	1.518	0.00113
0.65	1.530	0.00160	1.17	1.518	0.00114
0.66	1.530	0.00155	1.18	1.518	0.00114
0.67	1.529	0.00150	1.19	1.518	0.00115
0.68	1.529	0.00147	1.20	1.518	0.00115
0.69	1.528	0.00145	1.21	1.518	0.00115
0.70	1.528	0.00142	1.22	1.518	0.00115
0.71	1.527	0.00140	1.23	1.518	0.00115

Table I (continued)

λ (μm)	*n*	*k*	λ (μm)	*n*	*k*
1.24	1.518	0.00116	1.76	1.515	0.00128
1.25	1.518	0.00116	1.77	1.515	0.00129
1.26	1.518	0.00116	1.78	1.515	0.00129
1.27	1.517	0.00116	1.79	1.515	0.00129
1.28	1.517	0.00117	1.80	1.515	0.00130
1.29	1.517	0.00117	1.81	1.515	0.00130
1.30	1.517	0.00117	1.82	1.515	0.00130
1.31	1.517	0.00117	1.83	1.515	0.00131
1.32	1.517	0.00117	1.84	1.515	0.00131
1.33	1.517	0.00117	1.85	1.515	0.00132
1.34	1.517	0.00117	1.86	1.515	0.00132
1.35	1.517	0.00117	1.87	1.515	0.00133
1.36	1.517	0.00117	1.88	1.515	0.00134
1.37	1.517	0.00118	1.89	1.515	0.00134
1.38	1.517	0.00118	1.90	1.515	0.00135
1.39	1.517	0.00118	1.91	1.515	0.00135
1.40	1.517	0.00118	1.92	1.515	0.00136
1.41	1.517	0.00118	1.93	1.515	0.00137
1.42	1.517	0.00118	1.94	1.515	0.00137
1.43	1.517	0.00119	1.95	1.515	0.00138
1.44	1.517	0.00119	1.96	1.515	0.00138
1.45	1.516	0.00119	1.97	1.515	0.00139
1.46	1.516	0.00119	1.98	1.515	0.00140
1.47	1.516	0.00119	1.99	1.515	0.00141
1.48	1.516	0.00119	2.00	1.515	0.00142
1.49	1.516	0.00119	2.01	1.515	0.00142
1.50	1.516	0.00119	2.02	1.515	0.00143
1.51	1.516	0.00119	2.03	1.515	0.00144
1.52	1.516	0.00120	2.04	1.515	0.00144
1.53	1.516	0.00120	2.05	1.515	0.00145
1.54	1.516	0.00120	2.06	1.515	0.00146
1.55	1.516	0.00120	2.07	1.515	0.00147
1.56	1.516	0.00121	2.08	1.515	0.00149
1.57	1.516	0.00121	2.09	1.515	0.00150
1.58	1.516	0.00121	2.10	1.515	0.00152
1.59	1.516	0.00121	2.11	1.515	0.00153
1.60	1.516	0.00122	2.12	1.515	0.00154
1.61	1.516	0.00122	2.13	1.515	0.00155
1.62	1.516	0.00123	2.14	1.515	0.00155
1.63	1.516	0.00123	2.15	1.515	0.00156
1.64	1.516	0.00123	2.16	1.515	0.00156
1.65	1.516	0.00124	2.17	1.515	0.00156
1.66	1.516	0.00124	2.18	1.515	0.00157
1.67	1.516	0.00124	2.19	1.515	0.00157
1.68	1.516	0.00125	2.20	1.515	0.00158
1.69	1.516	0.00125	2.21	1.515	0.00158
1.70	1.516	0.00126	2.22	1.515	0.00159
1.71	1.516	0.00126	2.23	1.515	0.00159
1.72	1.516	0.00126	2.24	1.515	0.00160
1.73	1.516	0.00127	2.25	1.515	0.00160
1.74	1.516	0.00127	2.26	1.515	0.00160
1.75	1.515	0.00128	2.27	1.515	0.00161

Table I (continued)

λ (μm)	*n*	*k*	λ (μm)	*n*	*k*
2.28	1.515	0.00161	2.40	1.515	0.00165
2.29	1.515	0.00162	2.41	1.515	0.00165
2.30	1.515	0.00162	2.42	1.515	0.00165
2.31	1.515	0.00162	2.43	1.515	0.00165
2.32	1.515	0.00163	2.44	1.515	0.00165
2.33	1.515	0.00163	2.45	1.515	0.00165
2.34	1.515	0.00164	2.46	1.515	0.00165
2.35	1.515	0.00164	2.47	1.515	0.00165
2.36	1.515	0.00164	2.48	1.515	0.00166
2.37	1.515	0.00164	2.49	1.515	0.00166
2.38	1.515	0.00164	2.50	1.515	0.00166
2.39	1.515	0.00165			

Table II. Real (*n*) and imaginary (*k*) parts of the complex refractive index of kaolin.

λ (μm)	*n*	*k*	λ (μm)	*n*	*k*
0.13	1.757	0.310	0.65	1.566	0.00660
0.14	1.743	0.224	0.66	1.566	0.00660
0.15	1.697	0.151	0.67	1.565	0.00660
0.16	1.633	0.129	0.68	1.565	0.00660
0.17	1.577	0.142	0.69	1.565	0.00660
0.18	1.544	0.192	0.70	1.564	0.00660
0.19	1.562	0.270	0.71	1.564	0.00660
0.20	1.678	0.325	0.72	1.564	0.00660
0.21	1.760	0.214	0.73	1.564	0.00660
0.22	1.753	0.151	0.74	1.564	0.00660
0.23	1.741	0.110	0.75	1.563	0.00660
0.24	1.724	0.0752	0.76	1.563	0.00658
0.25	1.705	0.0560	0.77	1.563	0.00655
0.26	1.687	0.0412	0.78	1.563	0.00653
0.27	1.672	0.0332	0.79	1.562	0.00650
0.28	1.660	0.0278	0.80	1.562	0.00650
0.29	1.651	0.0221	0.81	1.562	0.00650
0.30	1.641	0.0181	0.82	1.562	0.00650
0.31	1.633	0.0151	0.83	1.562	0.00650
0.32	1.626	0.0130	0.84	1.562	0.00649
0.33	1.620	0.0117	0.85	1.562	0.00641
0.34	1.615	0.0105	0.86	1.562	0.00640
0.35	1.610	0.00957	0.87	1.562	0.00640
0.36	1.606	0.00867	0.88	1.561	0.00640
0.37	1.603	0.00762	0.89	1.561	0.00637
0.38	1.600	0.00661	0.90	1.561	0.00631
0.39	1.596	0.00597	0.91	1.561	0.00630
0.40	1.593	0.00551	0.92	1.561	0.00627
0.41	1.590	0.00526	0.93	1.561	0.00623
0.42	1.588	0.00522	0.94	1.561	0.00620
0.43	1.585	0.00530	0.95	1.561	0.00620
0.44	1.583	0.00540	0.96	1.561	0.00617
0.45	1.581	0.00550	0.97	1.561	0.00611
0.46	1.580	0.00565	0.98	1.561	0.00610
0.47	1.578	0.00579	0.99	1.560	0.00610
0.48	1.577	0.00590	1.00	1.560	0.00610
0.49	1.576	0.00600	1.01	1.560	0.00604
0.50	1.575	0.00610	1.02	1.560	0.00600
0.51	1.574	0.00619	1.03	1.560	0.00600
0.52	1.573	0.00627	1.04	1.560	0.00596
0.53	1.572	0.00632	1.05	1.560	0.00590
0.54	1.572	0.00636	1.06	1.560	0.00590
0.55	1.571	0.00641	1.07	1.560	0.00590
0.56	1.570	0.00645	1.08	1.560	0.00590
0.57	1.569	0.00648	1.09	1.560	0.00589
0.58	1.569	0.00652	1.10	1.560	0.00584
0.59	1.568	0.00656	1.11	1.560	0.00578
0.60	1.568	0.00660	1.12	1.560	0.00573
0.61	1.567	0.00660	1.13	1.560	0.00569
0.62	1.567	0.00660	1.14	1.560	0.00565
0.63	1.567	0.00660	1.15	1.560	0.00562
0.64	1.566	0.00660	1.16	1.560	0.00561

Table II (continued)

λ (μm)	*n*	*k*	λ (μm)	*n*	*k*
1.17	1.560	0.00560	1.69	1.559	0.00396
1.18	1.560	0.00555	1.70	1.559	0.00395
1.19	1.560	0.00551	1.71	1.559	0.00393
1.20	1.560	0.00550	1.72	1.559	0.00391
1.21	1.560	0.00550	1.73	1.559	0.00387
1.22	1.560	0.00548	1.74	1.559	0.00383
1.23	1.560	0.00544	1.75	1.559	0.00378
1.24	1.560	0.00540	1.76	1.559	0.00374
1.25	1.560	0.00536	1.77	1.559	0.00370
1.26	1.560	0.00532	1.78	1.559	0.00368
1.27	1.560	0.00528	1.79	1.559	0.00366
1.28	1.560	0.00524	1.80	1.559	0.00365
1.29	1.560	0.00520	1.81	1.559	0.00363
1.30	1.559	0.00520	1.82	1.559	0.00361
1.31	1.559	0.00520	1.83	1.559	0.00358
1.32	1.559	0.00520	1.84	1.559	0.00354
1.33	1.559	0.00516	1.85	1.559	0.00350
1.34	1.559	0.00513	1.86	1.559	0.00346
1.35	1.559	0.00509	1.87	1.559	0.00343
1.36	1.559	0.00506	1.88	1.559	0.00340
1.37	1.559	0.00502	1.89	1.559	0.00338
1.38	1.559	0.00499	1.90	1.559	0.00336
1.39	1.559	0.00496	1.91	1.559	0.00335
1.40	1.559	0.00493	1.92	1.559	0.00333
1.41	1.559	0.00490	1.93	1.559	0.00332
1.42	1.559	0.00487	1.94	1.559	0.00329
1.43	1.559	0.00483	1.95	1.559	0.00327
1.44	1.559	0.00480	1.96	1.559	0.00323
1.45	1.559	0.00478	1.97	1.559	0.00320
1.46	1.559	0.00475	1.98	1.559	0.00317
1.47	1.559	0.00472	1.99	1.559	0.00313
1.48	1.559	0.00469	2.00	1.559	0.00310
1.49	1.559	0.00466	2.01	1.559	0.00306
1.50	1.559	0.00463	2.02	1.559	0.00302
1.51	1.559	0.00461	2.03	1.559	0.00298
1.52	1.559	0.00458	2.04	1.559	0.00294
1.53	1.559	0.00455	2.05	1.559	0.00290
1.54	1.559	0.00453	2.06	1.559	0.00286
1.55	1.559	0.00450	2.07	1.559	0.00283
1.56	1.559	0.00447	2.08	1.559	0.00280
1.57	1.559	0.00445	2.09	1.559	0.00278
1.58	1.559	0.00442	2.10	1.559	0.00276
1.59	1.559	0.00440	2.11	1.559	0.00275
1.60	1.559	0.00435	2.12	1.559	0.00273
1.61	1.559	0.00430	2.13	1.559	0.00271
1.62	1.559	0.00425	2.14	1.559	0.00270
1.63	1.559	0.00421	2.15	1.559	0.00268
1.64	1.559	0.00416	2.16	1.559	0.00267
1.65	1.559	0.00411	2.17	1.559	0.00266
1.66	1.559	0.00407	2.18	1.559	0.00265
1.67	1.559	0.00402	2.19	1.559	0.00263
1.68	1.559	0.00399	2.20	1.559	0.00262

Table II (continued)

λ (μm)	*n*	*k*	λ (μm)	*n*	*k*
2.21	1.559	0.00261	2.36	1.559	0.00239
2.22	1.559	0.00259	2.37	1.559	0.00239
2.23	1.559	0.00257	2.38	1.559	0.00240
2.24	1.559	0.00254	2.39	1.559	0.00240
2.25	1.559	0.00251	2.40	1.559	0.00241
2.26	1.559	0.00249	2.41	1.559	0.00242
2.27	1.559	0.00246	2.42	1.559	0.00242
2.28	1.559	0.00243	2.43	1.559	0.00243
2.29	1.559	0.00241	2.44	1.559	0.00244
2.30	1.559	0.00240	2.45	1.559	0.00246
2.31	1.559	0.00239	2.46	1.559	0.00247
2.32	1.559	0.00238	2.47	1.559	0.00248
2.33	1.559	0.00238	2.48	1.559	0.00250
2.34	1.559	0.00238	2.49	1.559	0.00251
2.35	1.559	0.00239	2.50	1.559	0.00253

Table III. Real (n) and imaginary (k) parts of the complex refractive index of separated coats of *B. subtilis* spores.

λ (μm)	n	k	λ (μm)	n	k
0.20	1.637	0.0498	0.72	1.530	0.0147
0.21	1.617	0.0457	0.73	1.530	0.0145
0.22	1.604	0.0430	0.74	1.530	0.0143
0.23	1.594	0.0410	0.75	1.530	0.0141
0.24	1.586	0.0370	0.76	1.529	0.0139
0.25	1.578	0.0351	0.77	1.529	0.0138
0.26	1.572	0.0347	0.78	1.529	0.0136
0.27	1.567	0.0339	0.79	1.529	0.0134
0.28	1.563	0.0334	0.80	1.529	0.0133
0.29	1.560	0.0325	0.81	1.529	0.0132
0.30	1.557	0.0313	0.82	1.529	0.0130
0.31	1.555	0.0302	0.83	1.529	0.0128
0.32	1.552	0.0294	0.84	1.528	0.0127
0.33	1.550	0.0289	0.85	1.528	0.0126
0.34	1.548	0.0282	0.86	1.528	0.0124
0.35	1.547	0.0277	0.87	1.528	0.0124
0.36	1.545	0.0270	0.88	1.528	0.0122
0.37	1.544	0.0264	0.89	1.528	0.0121
0.38	1.543	0.0260	0.90	1.528	0.0120
0.39	1.542	0.0254	0.91	1.528	0.0118
0.40	1.541	0.0249	0.92	1.528	0.0117
0.41	1.540	0.0243	0.93	1.528	0.0116
0.42	1.539	0.0236	0.94	1.527	0.0116
0.43	1.539	0.0234	0.95	1.528	0.0114
0.44	1.538	0.0230	0.96	1.527	0.0113
0.45	1.538	0.0225	0.97	1.527	0.0113
0.46	1.537	0.0219	0.98	1.527	0.0112
0.47	1.536	0.0214	0.99	1.527	0.0110
0.48	1.536	0.0211	1.00	1.527	0.0109
0.49	1.535	0.0207	1.01	1.527	0.0108
0.50	1.535	0.0202	1.02	1.527	0.0107
0.51	1.534	0.0199	1.03	1.527	0.0107
0.52	1.534	0.0196	1.04	1.527	0.0106
0.53	1.534	0.0193	1.05	1.527	0.0106
0.54	1.533	0.0191	1.06	1.527	0.0105
0.55	1.533	0.0188	1.07	1.527	0.0104
0.56	1.533	0.0185	1.08	1.527	0.0104
0.57	1.532	0.0182	1.09	1.527	0.0104
0.58	1.532	0.0180	1.10	1.527	0.0102
0.59	1.532	0.0177	1.11	1.527	0.0101
0.60	1.532	0.0174	1.12	1.527	0.0100
0.61	1.532	0.0172	1.13	1.526	0.00994
0.62	1.531	0.0169	1.14	1.526	0.00987
0.63	1.531	0.0167	1.15	1.526	0.00981
0.64	1.531	0.0164	1.16	1.526	0.00975
0.65	1.531	0.0162	1.17	1.526	0.00970
0.66	1.531	0.0160	1.18	1.526	0.00969
0.67	1.531	0.0157	1.19	1.526	0.00969
0.68	1.530	0.0155	1.20	1.526	0.00961
0.69	1.530	0.0153	1.21	1.526	0.00950
0.70	1.530	0.0151	1.22	1.526	0.00942
0.71	1.530	0.0149	1.23	1.526	0.00935

Table III (continued)

λ (μm)	*n*	*k*	λ (μm)	*n*	*k*
1.24	1.526	0.00930	1.76	1.525	0.00799
1.25	1.526	0.00930	1.77	1.525	0.00799
1.26	1.526	0.00931	1.78	1.524	0.00796
1.27	1.526	0.00928	1.79	1.524	0.00791
1.28	1.526	0.00924	1.80	1.524	0.00786
1.29	1.526	0.00921	1.81	1.524	0.00782
1.30	1.526	0.00917	1.82	1.524	0.00778
1.31	1.526	0.00913	1.83	1.524	0.00775
1.32	1.526	0.00910	1.84	1.524	0.00773
1.33	1.526	0.00906	1.85	1.524	0.00771
1.34	1.526	0.00901	1.86	1.524	0.00770
1.35	1.526	0.00896	1.87	1.524	0.00769
1.36	1.526	0.00890	1.88	1.524	0.00769
1.37	1.525	0.00884	1.89	1.524	0.00769
1.38	1.525	0.00879	1.90	1.524	0.00770
1.39	1.525	0.00876	1.91	1.524	0.00771
1.40	1.525	0.00873	1.92	1.524	0.00771
1.41	1.525	0.00871	1.93	1.524	0.00772
1.42	1.525	0.00868	1.94	1.524	0.00772
1.43	1.525	0.00866	1.95	1.524	0.00773
1.44	1.525	0.00864	1.96	1.524	0.00773
1.45	1.525	0.00861	1.97	1.524	0.00774
1.46	1.525	0.00859	1.98	1.524	0.00774
1.47	1.525	0.00856	1.99	1.524	0.00775
1.48	1.525	0.00853	2.00	1.524	0.00775
1.49	1.525	0.00850	2.01	1.524	0.00775
1.50	1.525	0.00846	2.02	1.524	0.00774
1.51	1.525	0.00843	2.03	1.524	0.00773
1.52	1.525	0.00838	2.04	1.524	0.00773
1.53	1.525	0.00832	2.05	1.524	0.00771
1.54	1.525	0.00825	2.06	1.524	0.00770
1.55	1.525	0.00820	2.07	1.524	0.00768
1.56	1.525	0.00817	2.08	1.524	0.00766
1.57	1.525	0.00814	2.09	1.524	0.00764
1.58	1.525	0.00812	2.10	1.524	0.00761
1.59	1.525	0.00810	2.11	1.524	0.00758
1.60	1.525	0.00810	2.12	1.524	0.00755
1.61	1.525	0.00810	2.13	1.524	0.00753
1.62	1.525	0.00811	2.14	1.523	0.00753
1.63	1.525	0.00810	2.15	1.523	0.00754
1.64	1.525	0.00808	2.16	1.523	0.00757
1.65	1.525	0.00806	2.17	1.523	0.00760
1.66	1.525	0.00803	2.18	1.523	0.00764
1.67	1.525	0.00801	2.19	1.523	0.00767
1.68	1.525	0.00800	2.20	1.523	0.00771
1.69	1.525	0.00800	2.21	1.523	0.00774
1.70	1.525	0.00800	2.22	1.523	0.00778
1.71	1.525	0.00800	2.23	1.523	0.00782
1.72	1.525	0.00800	2.24	1.523	0.00786
1.73	1.525	0.00800	2.25	1.523	0.00791
1.74	1.525	0.00800	2.26	1.523	0.00795
1.75	1.525	0.00800	2.27	1.523	0.00800

Table III (continued)

λ (μm)	*n*	*k*	λ (μm)	*n*	*k*
2.28	1.523	0.00804	2.40	1.522	0.00836
2.29	1.523	0.00808	2.41	1.522	0.00847
2.30	1.523	0.00811	2.42	1.522	0.00858
2.31	1.523	0.00813	2.43	1.522	0.00872
2.32	1.523	0.00815	2.44	1.522	0.00886
2.33	1.523	0.00816	2.45	1.522	0.00902
2.34	1.523	0.00816	2.46	1.522	0.00919
2.35	1.522	0.00817	2.47	1.522	0.00938
2.36	1.522	0.00817	2.48	1.522	0.00958
2.37	1.522	0.00817	2.49	1.522	0.00979
2.38	1.522	0.00820	2.50	1.522	0.00999
2.39	1.522	0.00827			

Table IV. Real (n) and imaginary (k) parts of the complex refractive index of separated cores of *B. subtilis* spores.

λ (μm)	n	k	λ (μm)	n	k
0.20	1.734	0.195	0.72	1.518	0.00387
0.21	1.721	0.0991	0.73	1.518	0.00381
0.22	1.688	0.0735	0.74	1.518	0.00376
0.23	1.669	0.0491	0.75	1.518	0.00372
0.24	1.643	0.0282	0.76	1.517	0.00370
0.25	1.614	0.0261	0.77	1.517	0.00369
0.26	1.601	0.0369	0.78	1.517	0.00369
0.27	1.605	0.0408	0.79	1.517	0.00367
0.28	1.608	0.0281	0.80	1.517	0.00363
0.29	1.598	0.0132	0.81	1.517	0.00360
0.30	1.585	0.0106	0.82	1.516	0.00355
0.31	1.577	0.00990	0.83	1.516	0.00347
0.32	1.570	0.00930	0.84	1.516	0.00347
0.33	1.565	0.00881	0.85	1.516	0.00341
0.34	1.560	0.00876	0.86	1.515	0.00340
0.35	1.557	0.00841	0.87	1.515	0.00338
0.36	1.554	0.00808	0.88	1.515	0.00333
0.37	1.550	0.00763	0.89	1.515	0.00330
0.38	1.548	0.00760	0.90	1.515	0.00329
0.39	1.545	0.00742	0.91	1.515	0.00326
0.40	1.543	0.00721	0.92	1.515	0.00322
0.41	1.541	0.00696	0.93	1.514	0.00320
0.42	1.540	0.00670	0.94	1.514	0.00319
0.43	1.538	0.00660	0.95	1.514	0.00309
0.44	1.537	0.00650	0.96	1.514	0.00307
0.45	1.535	0.00639	0.97	1.514	0.00308
0.46	1.534	0.00612	0.98	1.514	0.00305
0.47	1.533	0.00591	0.99	1.514	0.00303
0.48	1.532	0.00578	1.00	1.514	0.00300
0.49	1.530	0.00565	1.01	1.513	0.00298
0.50	1.529	0.00551	1.02	1.513	0.00296
0.51	1.529	0.00538	1.03	1.513	0.00297
0.52	1.528	0.00527	1.04	1.513	0.00295
0.53	1.527	0.00516	1.05	1.513	0.00291
0.54	1.526	0.00505	1.06	1.513	0.00291
0.55	1.526	0.00496	1.07	1.513	0.00291
0.56	1.525	0.00487	1.08	1.513	0.00289
0.57	1.525	0.00479	1.09	1.513	0.00287
0.58	1.524	0.00472	1.10	1.513	0.00285
0.59	1.524	0.00466	1.11	1.513	0.00282
0.60	1.523	0.00459	1.12	1.513	0.00281
0.61	1.522	0.00453	1.13	1.512	0.00279
0.62	1.522	0.00447	1.14	1.512	0.00278
0.63	1.522	0.00442	1.15	1.512	0.00276
0.64	1.521	0.00436	1.16	1.512	0.00275
0.65	1.521	0.00430	1.17	1.512	0.00274
0.66	1.520	0.00424	1.18	1.512	0.00273
0.67	1.520	0.00418	1.19	1.512	0.00272
0.68	1.520	0.00411	1.20	1.512	0.00271
0.69	1.519	0.00405	1.21	1.512	0.00270
0.70	1.519	0.00398	1.22	1.512	0.00269
0.71	1.519	0.00392	1.23	1.512	0.00268

Table IV (continued)

λ (μm)	n	k	λ (μm)	n	k
1.24	1.512	0.00267	1.76	1.510	0.00231
1.25	1.512	0.00266	1.77	1.510	0.00230
1.26	1.512	0.00265	1.78	1.510	0.00230
1.27	1.512	0.00264	1.79	1.510	0.00229
1.28	1.512	0.00263	1.80	1.510	0.00229
1.29	1.512	0.00262	1.81	1.510	0.00228
1.30	1.512	0.00261	1.82	1.510	0.00228
1.31	1.512	0.00261	1.83	1.510	0.00227
1.32	1.511	0.00260	1.84	1.510	0.00227
1.33	1.511	0.00259	1.85	1.510	0.00226
1.34	1.511	0.00259	1.86	1.510	0.00226
1.35	1.511	0.00258	1.87	1.510	0.00225
1.36	1.511	0.00257	1.88	1.510	0.00225
1.37	1.511	0.00257	1.89	1.510	0.00225
1.38	1.511	0.00256	1.90	1.510	0.00225
1.39	1.511	0.00256	1.91	1.510	0.00225
1.40	1.511	0.00255	1.92	1.510	0.00225
1.41	1.511	0.00254	1.93	1.510	0.00225
1.42	1.511	0.00254	1.94	1.510	0.00225
1.43	1.511	0.00253	1.95	1.510	0.00226
1.44	1.511	0.00252	1.96	1.510	0.00226
1.45	1.511	0.00252	1.97	1.510	0.00227
1.46	1.511	0.00251	1.98	1.510	0.00227
1.47	1.511	0.00250	1.99	1.510	0.00228
1.48	1.511	0.00250	2.00	1.510	0.00228
1.49	1.511	0.00249	2.01	1.510	0.00228
1.50	1.511	0.00248	2.02	1.510	0.00229
1.51	1.511	0.00248	2.03	1.510	0.00229
1.52	1.511	0.00247	2.04	1.510	0.00230
1.53	1.511	0.00246	2.05	1.510	0.00230
1.54	1.511	0.00245	2.06	1.510	0.00231
1.55	1.510	0.00245	2.07	1.510	0.00231
1.56	1.510	0.00244	2.08	1.510	0.00232
1.57	1.510	0.00243	2.09	1.510	0.00232
1.58	1.510	0.00242	2.10	1.510	0.00233
1.59	1.510	0.00241	2.11	1.510	0.00233
1.60	1.510	0.00241	2.12	1.510	0.00234
1.61	1.510	0.00240	2.13	1.510	0.00235
1.62	1.510	0.00239	2.14	1.510	0.00235
1.63	1.510	0.00238	2.15	1.510	0.00236
1.64	1.510	0.00237	2.16	1.510	0.00237
1.65	1.510	0.00237	2.17	1.510	0.00237
1.66	1.510	0.00236	2.18	1.510	0.00238
1.67	1.510	0.00235	2.19	1.510	0.00239
1.68	1.510	0.00235	2.20	1.510	0.00240
1.69	1.510	0.00234	2.21	1.510	0.00241
1.70	1.510	0.00234	2.22	1.510	0.00242
1.71	1.510	0.00233	2.23	1.510	0.00243
1.72	1.510	0.00233	2.24	1.510	0.00244
1.73	1.510	0.00232	2.25	1.510	0.00245
1.74	1.510	0.00232	2.26	1.510	0.00246
1.75	1.510	0.00231	2.27	1.510	0.00247

Table IV (continued)

λ (μm)	*n*	*k*	λ (μm)	*n*	*k*
2.28	1.510	0.00248	2.40	1.510	0.00265
2.29	1.510	0.00249	2.41	1.510	0.00267
2.30	1.510	0.00251	2.42	1.510	0.00269
2.31	1.510	0.00252	2.43	1.510	0.00271
2.32	1.510	0.00253	2.44	1.510	0.00272
2.33	1.510	0.00255	2.45	1.510	0.00274
2.34	1.510	0.00256	2.46	1.510	0.00276
2.35	1.510	0.00257	2.47	1.510	0.00278
2.36	1.510	0.00259	2.48	1.510	0.00280
2.37	1.510	0.00260	2.49	1.510	0.00282
2.38	1.510	0.00262	2.50	1.510	0.00284
2.39	1.510	0.00264			

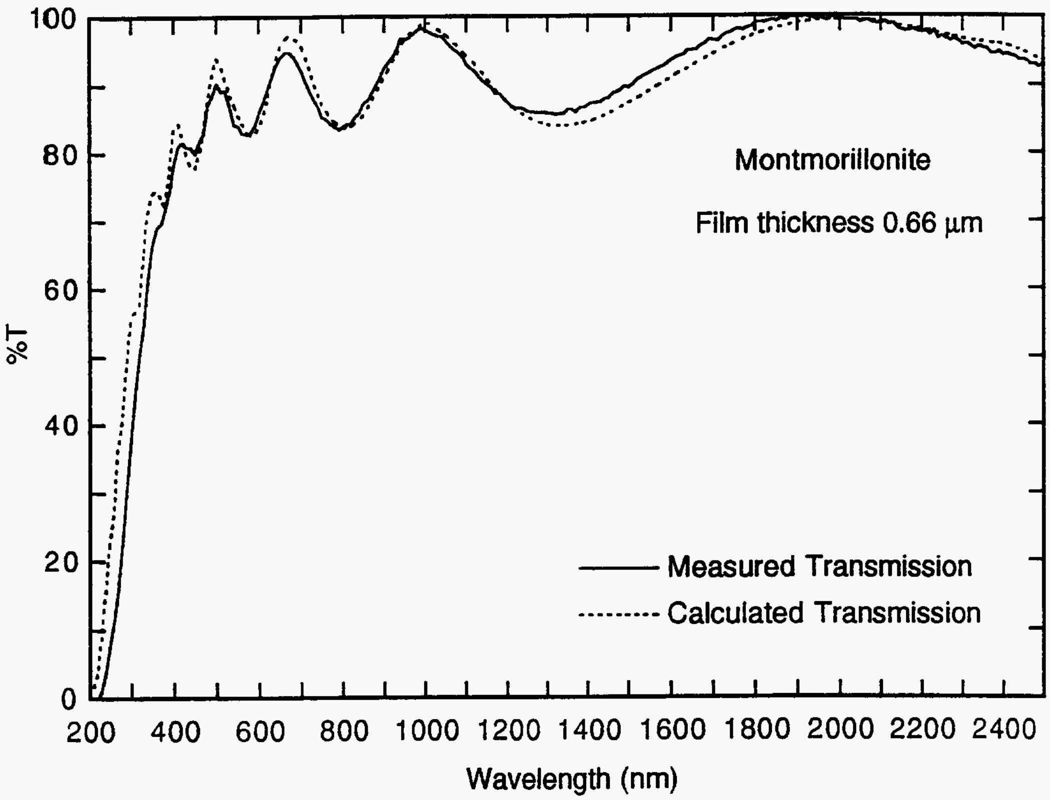

Figure 1. Transmission spectrum of a montmorillonite film 0.66 μm thick. The theoretical transmittance, calculated using the measured optical constants, is also shown.

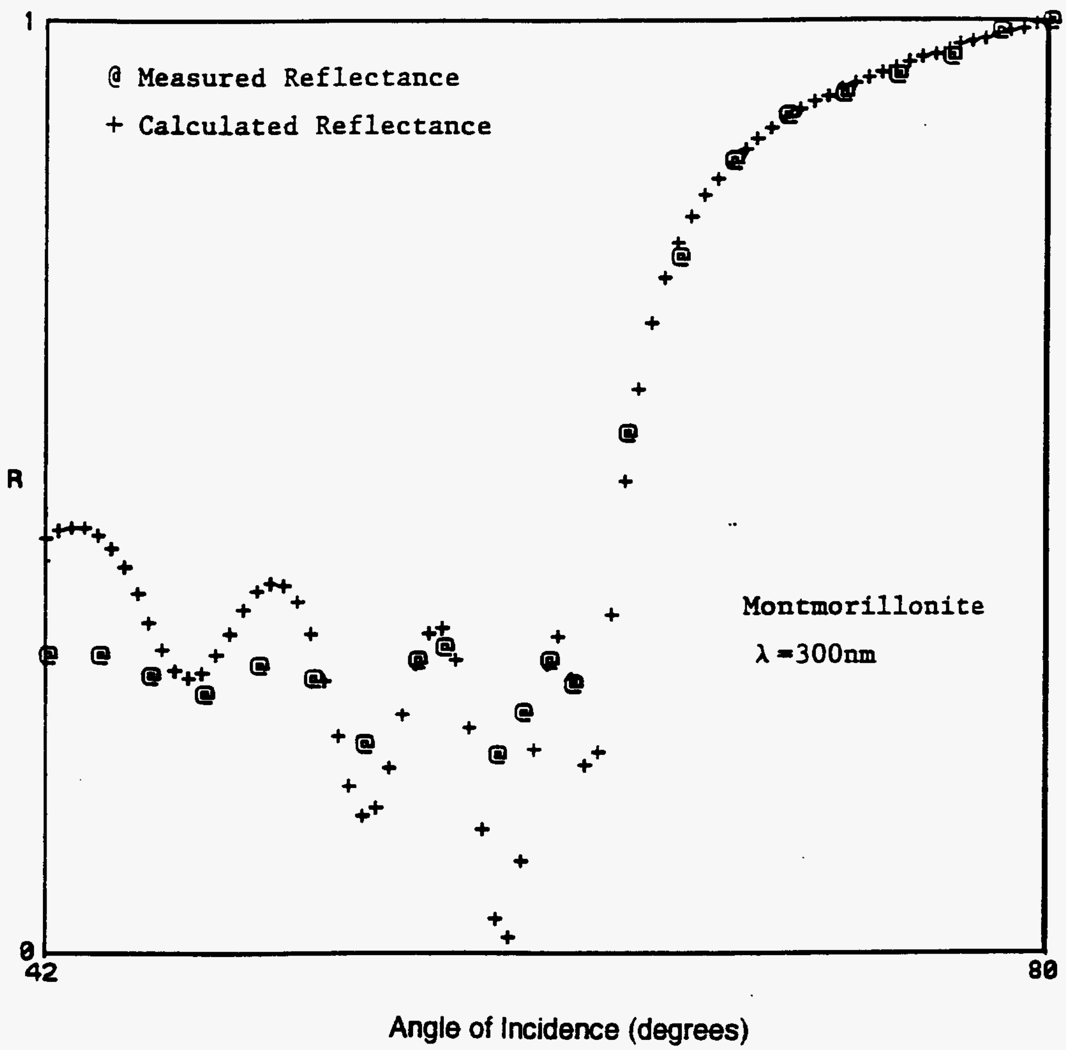

Figure 2. Reflectance spectrum obtained in a measurement of the index of refraction of montmorillonite using the critical-angle technique. The theoretical reflectance calculated using Fresnel's equations is also shown.

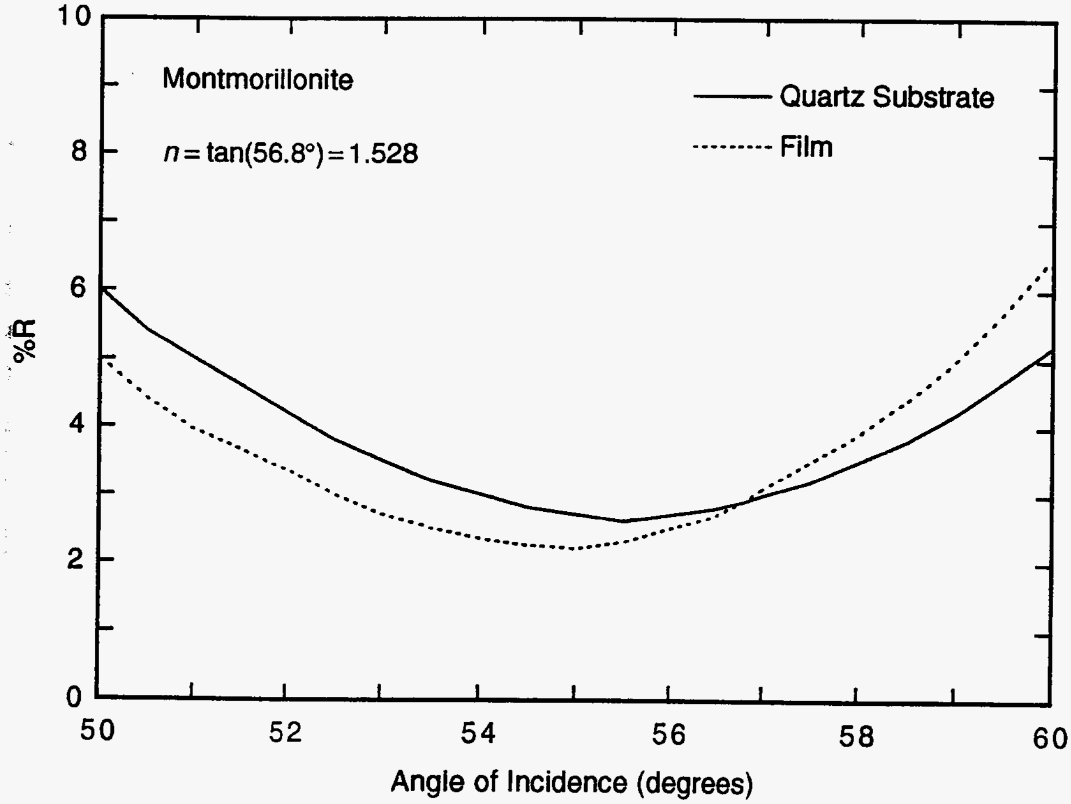

Figure 3. Reflectance spectra obtained in a measurement of the index of refraction of montmorillonite using Abeles' method. The wavelength is 500 nm.

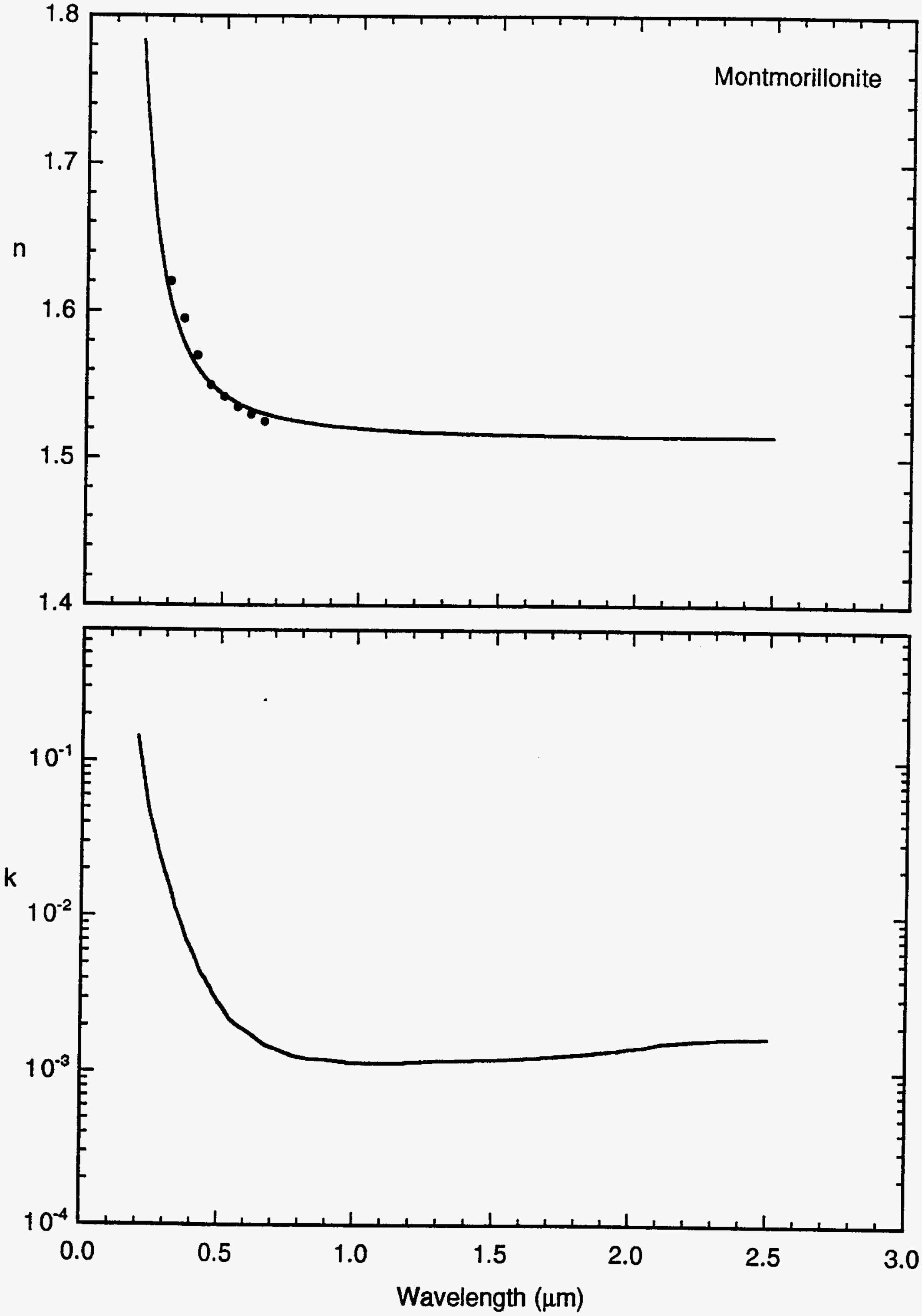

Figure 4. Optical constants of montmorillonite from 0.2 to 2.5 μm.

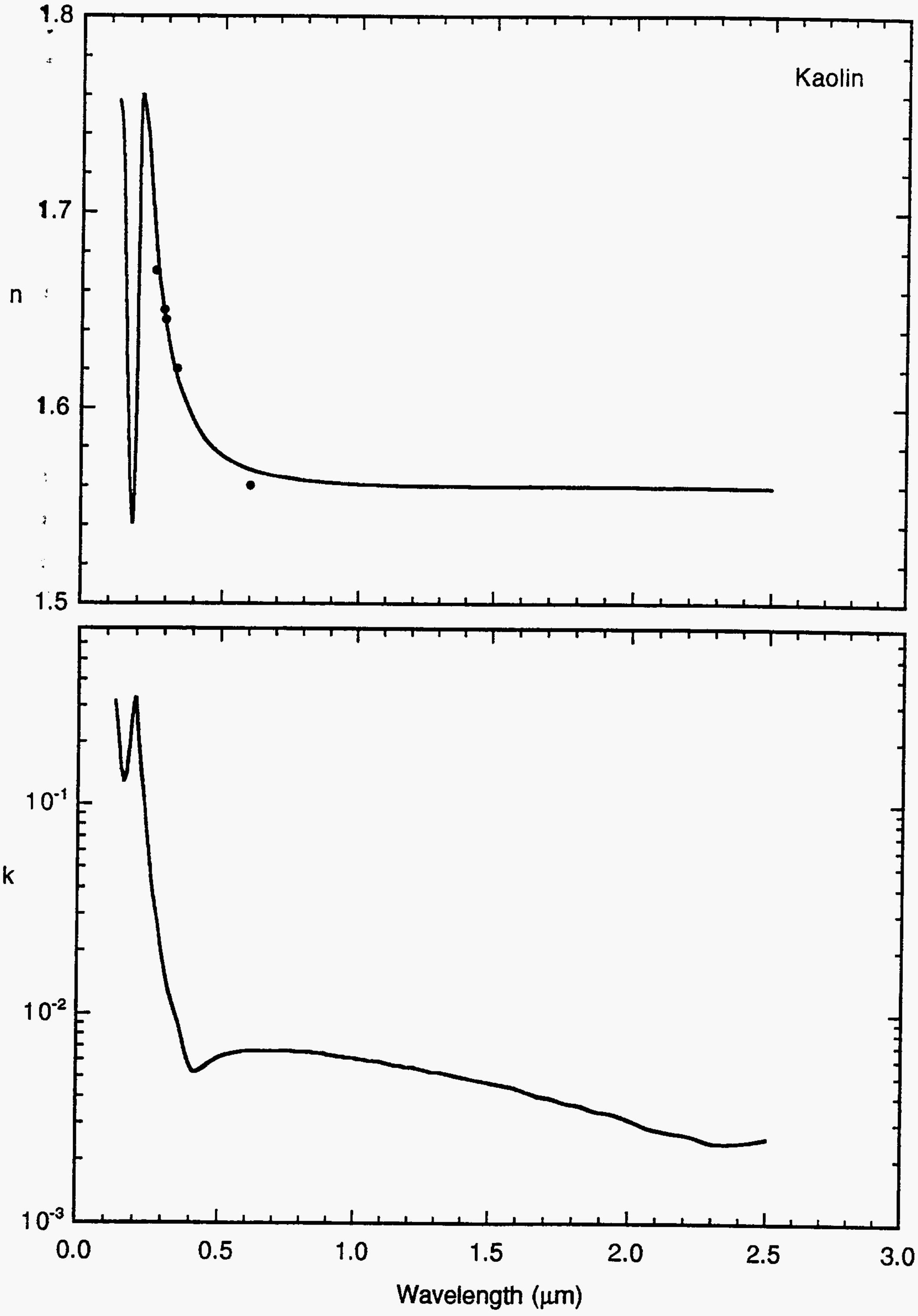

Figure 5. Optical constants of kaolin from 0.13 to 2.5 μm.

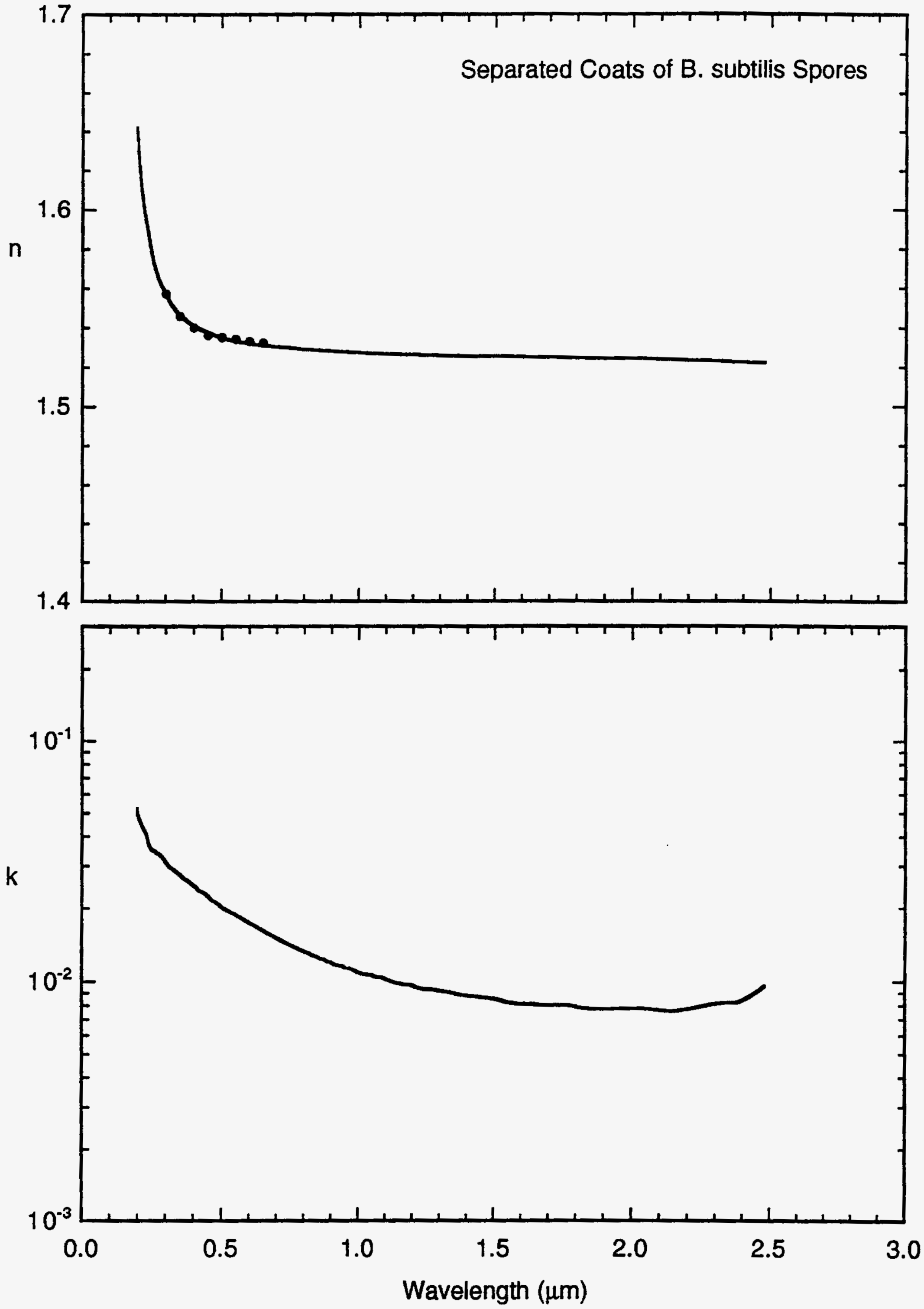

Figure 6. Optical constants of separated coats of B. subtilis spores from 0.2 to 2.5 μm.

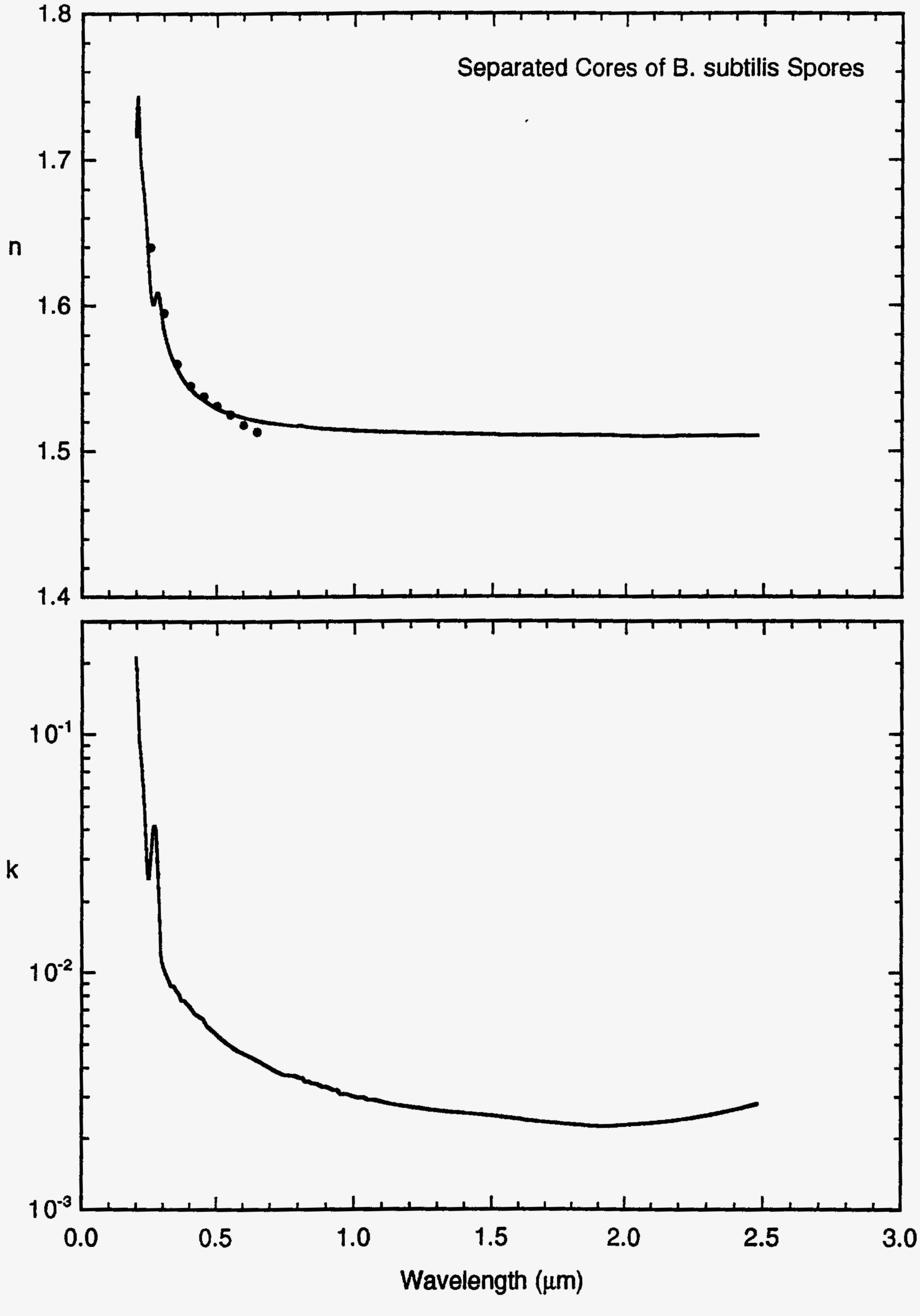

Figure 7. Optical constants of separated cores of B. subtilis spores from 0.2 to 2.5 µm.

M98001913

Report Number (14) ORNL/CP--95872
CONF-9706222--

Publ. Date (11) 199712
Sponsor Code (18) DOE/ER, XF
UC Category (19) UC-400, DOE/ER

DOE